Subglacial lake activity beneath the ablation zone of the Greenland Ice Sheet

Yubin Fan[1,2,3], Chang-Qing Ke[1,2,3*], Xiaoyi Shen[1,2,3], Yao Xiao[1,2,3], Stephen J. Livingstone[4], Andrew J. Sole[4]

[1]Jiangsu Provincial Key Laboratory of Geographic Information Science and Technology, Key Laboratory for Land Satellite Remote Sensing Applications of Ministry of Natural Resources, School of Geography and Ocean Science, Nanjing University, Nanjing, 210023 China.
[2]Collaborative Innovation Center of Novel Software Technology and Industrialization, Nanjing, 210023 China.
[3]Collaborative Innovation Center of South China Sea Studies, Nanjing, 210023 China.
[4] Geography Department, University of Sheffield, Sheffield, UK, S10 2TN.

Correspondence to: Chang-Qing Ke (kecq@nju.edu.cn)

Abstract. Hydrologically active subglacial lakes can drain large volumes of water and sediment along subglacial pathways, affecting the motion and mass balance of ice masses, and impacting downstream sediment dynamics. Only seven active lakes have been reported beneath the Greenland Ice Sheet (GrIS) to date, and thus a systematic understanding of their spatial distribution and dynamic processes is still lacking. Here, using ICESat-2 ATL11 data, we identify 61 active subglacial lakes, 59 of which have not been previously reported. Multi-temporal ArcticDEM strip maps were used to extend the timeseries to verify lakes and determine their drainage history. The identification of active subglacial lakes beneath the GrIS is complicated by the occurrence of supraglacial lakes, which also fill and drain, and are hypothesized to be almost co-located. We therefore used the temporal pattern and magnitude of ice-surface elevation change to discriminate subglacial lakes, and utilized the ability of ICESat-2 to penetrate through shallow surface water to correct the elevation provided by the ATL11 data. A significant localized elevation anomaly was still measured in all detected subglacial lakes after correction, revealing that 18 subglacial lakes are twinned with supraglacial lakes. The active subglacial lakes have large upstream hydrological catchments and are located near or below the equilibrium line. Lakes have an average area of 3.11 km^2, and most lake exhibited positive elevation/volume-change rate during the ICESat-2 period. These observations suggest that active subglacial lakes are widespread components of the Greenland subglacial drainage system and provide critical information for understanding their activity.

删除的内容: the
删除的内容: identified
删除的内容: However,
删除的内容: allowed us
删除的内容:

1 Introduction

Subglacial lakes that fill and drain on annual to decadal timescales are termed hydrologically active subglacial lakes (henceforth ‘active’). These lakes transiently store and then release water downstream, lubricating the ice-bed interface and affecting ice sheet mass balance by changing the ice discharge speed (Siegfried & Fricker, 2018; Malczyk et al., 2020). Some active subglacial lakes are hydraulically connected to other lakes, and water exchange between lakes can impact hydraulic gradients and subglacial water flow (Smith et al., 2017). Lake drainage not only exchanges water between lakes, but also

transfers sediment and nutrients downstream, feeding microbial communities (Vick-Majors et al., 2020). Water crossing the grounding line can also reduce the stability of ice shelves (Li et al., 2021). Therefore, knowledge of the distribution and water budget of active subglacial lakes is vital for understanding the stability of ice sheets.

Subglacial lakes can be identified from various remote sensing techniques. Gravity and seismic data using acoustic impedance or amplitude-versus-angle analysis can determine their bathymetries and characterize their geological properties (Studinger et al., 2004; Yan et al., 2022). Additionally, subglacial lakes produce a flat ice-bed interface with high reflectance in radargrams and can therefore be recognized from radar echo sounding (RES) (Wright et al., 2012; Palmer et al., 2013; Bowling et al., 2019; Bessette et al., 2021; Maguire et al., 2021). Water that moves in and out of subglacial lakes can lead to localized ice-sheet surface deformation, enabling the lakes' corresponding volume changes to be studied through localized elevation anomalies detected from satellite radar (Siegfried & Fricker, 2018), laser altimeters (Smith et al., 2009; Siegfried & Fricker, 2021), and multi-temporal optical (Palmer et al., 2015) and radar interferometry-based Digital Elevation Models (DEMs) (Gray et al., 2005).

More than 675 subglacial lakes have been detected underneath the Antarctic Ice Sheet (Livingstone et al., 2022), including more than 130 active lakes (Smith et al., 2009; 2017). Conversely, only 7 active and 57 stable subglacial lakes have been identified underneath the Greenland Ice Sheet (GrIS) (Livingstone et al., 2022), although hydrologic potential calculations indicate that subglacial lakes could account for approximately 1.2% of the GrIS area (Livingstone et al., 2013). Constrained by steeper ice surface slopes and thus stronger hydraulic gradients, lakes underneath the GrIS tend to be smaller (Bowling et al., 2019), making it difficult for satellite altimeters (e.g., ICESat and CryoSat-2) to study subglacial lake activity in detail due to their coarse spatial or temporal resolutions. The few active lakes underneath the GrIS that have been observed, were identified from multi-temporal DEMs (Palmer et al., 2015; Howat et al., 2015; Bowling et al., 2019; Livingstone et al., 2019).

ICESat-2 has an improved footprint size (approximately 11 m with 0.7 m along-track spacing) (Magruder et al., 2020) and spatial coverage (±88° latitudes) compared to previous satellite altimeters, providing an essential dataset for enabling active subglacial lake detection across the GrIS. Furthermore, its 91-day revisit cycle has the ability to reveal how the basal water system operates on sub-annual timescales. This study aims to detect active GrIS subglacial lakes by measuring ice-surface elevation anomalies observed from ICESat-2 between March 2019 and December 2020. Subglacial lakes were verified and their boundaries identified using the ArcticDEM (Porter et al. 2018). Spatial patterns of elevation and volume changes over the ICESat-2 period (2019-2020) were generated, and the elevation time-series over the combined ArcticDEM and ICESat-2 periods (2009-2020) were used to determine the temporal patterns of lake activity.

删除的内容: observations
删除的内容: Seismic
删除的内容: gravity inversions of lakes
删除的内容: their
删除的内容: height
删除的内容: 17
删除的内容: confirmed
删除的内容: ICESat-2 periods

2 Data

2.1 ICESat-2 data

The ATL11 product 'Slope-Corrected Land Ice Height Time Series' (Smith et al., 2021) is derived by correcting offsets between the reference ground track (RGT) and the location of ATL06 land ice measurements, and provides ice surface elevations with a 91-day cycle in polar regions (poleward of 60° N and 60° S), accompanied by geolocation information and the corresponding quality assessment. The three beam pairs of ICESat-2 follow a reference pair track (RPT) parallel to the RGT, with the reference points of the ATL11 product spaced along each RPT. The ATL11 product is posted at a spatial resolution of 60 m, with the spacing of tracks within each RPT ranging from approximately 5.4 km (high latitude) to 7.4 km (low latitude). More information on the ATL11 data and its processing algorithm can be found in Smith et al. (2021).

The ICESat-2 ATL11 v3 product contains ice surface elevations with respect to the WGS84 ellipsoid from March 2019 to December 2020 (i.e., cycles 3-9). In total, the elevation measurements of all 511 RGTs (1533 RPTs, 2638 track segments) were used to detect active subglacial lakes and explore their elevation and volume changes from 2019 to 2020. We collated 2.91×10^7 reference points over the Greenland Ice Sheet. Only data with cycles marked as good quality (quality_summary=0) were used, leading to an overall spatial density of 1.34×10^5 points per square kilometer. ATL06 and ATL11 products only capture the elevations of the top photons (and thus identify the ice or water surface only), but the ATL03 data contain the full stream of returned photons (Neumann et al., 2019), which were used to identify surface meltwater depths and correct the ice surface elevation measurements for its presence during the melt season.

2.2 Verification data

The ArcticDEM is a high-resolution, high-quality digital surface model (DSM) of the Arctic based on optical stereo imagery from GeoEye-1 and WorldView-1/2/3 (Porter et al., 2018), and with an internal accuracy of 0.2 m (Noh & Howat, 2015). The 2-m resolution strip DSM files provided time-stamped elevation measurements from August 2009 to March 2017. The temporal resolution of these time-stamped DSM segments was variable due to the influence of clouds and shadows. Nevertheless, the dataset enables the detection of localized elevation-change anomalies, and was used for lake cross-verification and boundary estimation. Published Greenland subglacial lake locations (Livingstone et al., 2022) were also used for verification.

3 Methods

3.1 Identification of active subglacial lakes

Subglacial lakes were detected from localized ice-surface elevation anomalies measured by ICESat-2. The elevation-change rate of individual reference points was obtained through a linear fit by using the timestamp and elevation value of valid

删除的内容: Time series of ice surface heights derived from the ICESat-2 ATL11 (Version 3) product (Smith et al., 2021) were used to study active subglacial lakes. The product contains

删除的内容: for repeat observations along each ICESat-2 reference ground track (RGT) from cycle to cycle (91 days apart)

删除的内容: RGT

删除的内容: for each reference point

删除的内容: collect

删除的内容: entire of Greenland

删除的内容: Finally,

删除的内容: , which

删除的内容: Validation

删除的内容: However, the time-stamped strip ArcticDEM

删除的内容: allows

删除的内容: validation

删除的内容: extraction

删除的内容: validation

删除的内容: height

elevation measurements (e.g., Figure 1a). We then generated a Greenland-wide elevation change trend map by gridding these point trend data at a resolution of 500 m, which covers approximately 80% of the GrIS. The change map was used to create masks for candidate regions. Previous studies in Antarctica used a threshold of ± 0.5 m/yr to select regions with a significant localized elevation change (Fricker et al., 2007; Smith et al., 2017; Malczyk et al., 2020), but knowledge of such a threshold applicable to Greenland subglacial lakes is lacking. We adopted a more conservative threshold of ± 0.2 m/yr to identify potential subglacial lakes that could then be verified using the ArcticDEM dataset and through manual examination of ice-surface elevation patterns.

The relative elevation-change anomaly associated with a subglacial lake should have a characteristic spatial pattern comprising an obvious elevation anomaly at the lake center which reduces to zero (within uncertainty) outside the lake. Candidate regions where such elevation anomalies can be explained by other factors, including displacement of the ICESat-2 footprints, dynamic topography, and cloud cover, etc., were discarded (Smith et al., 2009). The elevation profiles were used to determine lake location by visual interpretation (Willis et al., 2015) (e.g., Figures 1b, c).

3.2 ArcticDEM verification, lake boundary determination and lake activity recognition

Each of the DSMs was corrected against filtered ICESat altimetry data using the metadata provided, and time-series of time-stamped ArcticDEM data were used to cross-verify subglacial lake locations. Areas of known subglacial lakes in Greenland range from 0.18 to 8.4 km^2, with a maximum length of 1.6 km (Livingstone et al., 2022). Therefore, a 5 km radius circular buffer was established around the point at the center of the potential lake determined from the ICESat-2 data, which was taken as the maximum possible extent of the subglacial lake. To provide spatially continuous images and improve computational efficiency, we derived the median value of the DSMs every 100 days to obtain elevation maps. Then, we calculated the elevation difference between each temporally adjacent elevation map, which was used to determine whether there was an elevation anomaly (e.g., Figure 1a). Elevation anomalies identified in both the ICESat-2 and ArcticDEM data were confirmed as potential subglacial lakes (henceforth 'confirmed lakes'). We acknowledge that the time differences between ICESat-2 and ArcticDEM data might affect the percentage of confirmed lakes because some lakes did not exhibit complete drainage or filling activity. However, it allowed us to extend the temporal coverage of the data by 8 years, giving a more comprehensive picture of the patterns of elevation changes, which was critical for discriminating subglacial lakes from other processes. The large spacing of ICESat-2 tracks (5-7 km, exceeding the lake size) make it difficult to extract the subglacial lake boundary by generating an elevation-change surface through interpolation of the ICESat-2 data. Therefore, lake boundaries were manually delineated from the ArcticDEM elevation-change anomaly maps. We still retained subglacial lakes that were not identified from the ArcticDEM (henceforth 'unconfirmed lakes'), to analyze the spatial pattern and elevation-change rate, but eliminated them from our analysis of volume change and long-term lake activity.

Long time-series of elevation change were used to determine subglacial lake fill-drain patterns. To remove the influence of systematic vertical and horizontal offsets between ArcticDEMs, we calculated the relative elevation anomaly by subtracting

删除的内容: We did not interpolate the cells to reduce the potential misidentification of subglacial lakes.

删除的内容: in Antarctica

带格式的: 字体颜色: 自动设置

带格式的: 字体颜色: 自动设置

删除的内容: The elevation-change anomaly associated with subglacial lake filling and/ or drainage should have a characteristic spatial pattern comprising an obvious elevation anomaly at the lake center while the outside remains stable

删除的内容: the

删除的内容: anomaly

删除的内容: validation

删除的内容: and

删除的内容: T

删除的内容: validate

删除的内容: the

删除的内容: Subglacial lakes which also coincided with elevation anomalies during the ArcticDEM period were confirmed as subglacial lakes

删除的内容: show full

删除的内容:

删除的内容: the

删除的内容: boundary

删除的内容: was

the averaged ice-surface elevation within the lake outline from the buffer around it (Livingstone et al., 2019). We used the same method to calculate the relative elevation anomaly of ICESat-2, and then combined the ArcticDEM and ICESat-2 periods (2009-2020) to determine the temporal patterns of lake activity (e.g., Figure 1d). For calculating the relative elevation anomaly, we used the internal accuracy of the data as a measure of uncertainty. The internal accuracy of the ArcticDEM is 0.2 m (Noh & Howat, 2015), and 0.04 m for ICESat-2 footprints (Brunt et al., 2021).

3.3 Impact of supraglacial lakes on the detection of subglacial lakes

Numerous supraglacial lakes seasonally form in much of the ablation zone of the GrIS, and then either freeze or drain over the ice surface or to the bed (Selmes et al., 2011). The filling and drainage of these lakes produces ice-surface elevation anomalies in the ATL06 (i.e. land ice height) product (and therefore the ATL11 product) that could be mis-classified as subglacial lake activity. This is particularly challenging because supraglacial and subglacial lakes are hypothesized to exist in tandem (Sergienko, 2013). Moreover, if a subglacial lake located beneath the ablation zone drains, the ice-surface depression created would provide a natural basin for water to pond (Willis et al., 2015).

To discriminate between surface and subglacial lakes we first evaluated the temporal pattern and magnitude of the ice-surface elevation changes. Supraglacial lakes often drain rapidly to the bed in the summer via moulins (MacFerrin et al., 2019), and are therefore characterized by a seasonal fill-drain pattern, whereas subglacial lakes tend to fill over multiple years. Supraglacial lakes are also typically shallow features (Pope et al., 2016) and so large elevation anomalies (>10 m) are more likely to be caused by subglacial lake drainages. A key advantage of ICESat-2 is that the ATL03 photon data can penetrate surface meltwater as deep as 7 m (Fair et al., 2020) producing a double reflection of both the water surface and ice surface beneath (Fricker et al., 2020). For each potential subglacial lake, we were therefore able to identify whether there was a double reflection in the ATL03 profile. We also manually checked the Landsat-8 images around the acquisition time of ICESat-2 to further confirm the existence of surface water. We applied the Watta algorithm (Datta et al., 2021) to discriminate the supraglacial lake surface and bottom noting that this method does not work if the lake was covered with a frozen lid of ice. The bottom elevation was taken as the corrected ATL11 elevation and used to recalculate the elevation-change rate for subglacial lake footprints within each supraglacial lake (Figure S1). The Watta-derived depths show a high correlation with the image-based and manual-picked depths, and the depth uncertainty is small compared with the corresponding elevation change. This correction was applied to 18 subglacial lakes, and in all cases a significant localized elevation anomaly was still measured indicating that ~30% of active subglacial lakes in this study are twinned with supraglacial lakes.

3.4 Lake confidence level classification

We classified potential subglacial lakes into three confidence levels (e.g., Figure 2). Low confidence lakes exhibited no clear pattern of multi-year elevation change with time, might be associated with flat surfaces and annual elevation cycles that could be the expression of supraglacial lakes, had a limited number of data points, and a small maximum corrected elevation change

删除的内容:
删除的内容: surface
删除的内容: In
删除的内容: numerous supraglacial lakes seasonally form
删除的内容: and apply the Watta algorithm to discriminate the supraglacial lake surface and bottom (Datta et al., 2021)
删除的内容: height
删除的内容: elevation
删除的内容: surface
删除的内容: these
删除的内容: surface
删除的内容: signa
删除的内容: l

(<10 m change). High confidence lakes were identified from >10 m corrected ice-surface elevation change, had a clear double reflector or no evidence of surface water, and an elevation change pattern typical of subglacial lakes (e.g., multi-year pattern of filling and then rapid drainage). Medium confidence lakes had an elevation change pattern typical of subglacial lakes, but a less clear signal, for example a smaller ice-surface elevation change, fewer data points or some flat surfaces. We discounted the low confidence potential lakes as likely to be caused by other processes (e.g., filling and draining of supraglacial lakes).

3.5 Estimation of lake elevation and volume change

The elevation-change rate within the lake polygons is composed of ice-flux divergence, ice ablation and basal water motion (Smith et al., 2009), while the ice outside is only affected by ice-flux divergence and ablation. This 'background' elevation change needs to be subtracted to calculate the relative elevation-change caused by the subglacial lake. For each ICESat-2 overpass, we first calculated the median value of all ICESat-2 measurement points within the lake polygon, and then the median elevation of the area surrounding the lake (within the buffer-region) was subtracted to produce the elevation anomaly. To quantify the effect of buffer-region width on the calculated elevation-change rate, we tested three ring buffers which extended beyond the lake outline: buffer1, a fixed buffer of 2 km width; buffer2, a buffer with a width equal to the radius of a circle whose area is equal to the lake, and buffer3, with half the width of buffer2 (Table S1). The fixed 2km buffer exhibited a large difference compared to the adaptive ones because most lakes are smaller than 1 km^2. The mean value of the absolute differences between the two calculated elevation-change rates using adaptive buffers was approximately 0.16 m, which only accounts for 6.5% of the averaged absolute elevation-change rate. Therefore, the effect of the buffer size on the elevation-change rate was neglected, and buffer2 was applied because it is a similar footprint size to the lake region. For the unconfirmed lakes, we used half of the ICESat-2 along-track distance where the elevation anomaly was detected as a buffer.

We calculated the corrected elevation change rate, dh_c for each lake as shown in Equation 1:

$$dh_c = dh_{median,\text{inside}} - dh_{median,\text{outside}} \quad (1)$$

where $dh_{median,inside}$ is the median elevation-change rate of ATL11 footprints within each lake's bounding polygon, and $dh_{median,outside}$ is defined as the median value of the elevation change rate for ATL11 footprints outside the bounding polygon but within the buffer zone.

The uncertainty of the elevation-change rate was calculated by the standard deviation of the elevation-change rates of all footprints inside and outside the lake polygon, defined in Equation 2.

$$dh_{c,\text{uncertainty}} = \sqrt{dh^2_{std,inside} + dh^2_{std,outside}} \quad (2)$$

The volume change rate was derived by integrating the elevation change rate and lake boundary for the confirmed lakes (Equation 3). To estimate the errors in our volume change estimates caused by boundary migration, we assumed an area

删除的内容: surface

删除的内容:

删除的内容: 5

带格式的: 字体颜色: 自动设置

带格式的: 字体颜色: 自动设置

删除的内容: The median elevation-change rate during the ICESat-2 period was first calculated for all the lake polygons. As this rate is composed of ice-flux divergence, ice ablation and water motion (Smith et al., 2009), the median elevation-change rate of the area surrounding the lake (within a buffer-region) was subtracted to isolate the relative elevation-change effect of the subglacial lake.

删除的内容:

删除的内容: Here, we defined a circular buffer region outside each lake boundary with a width equal to the radius of a circle whose area is equal to the lake. To quantify the effect of buffer-region width on the elevation-change rate, we tested two other width buffers: (1) a fixed buffer of 2 km; and (2) a buffer of half the radius of the standard buffer (Table S1).

删除的内容: adapted

删除的内容:

删除的内容: A boundary that encompassed all elevation-change anomalies was then defined, and w

删除的内容: defined

删除的内容: the

删除的内容: s

uncertainty of one grid cell of the ArcticDEM differencing image (i.e., 30 m x 30 m) and calculated the volume change uncertainty as shown in Equation 4.

$$dV_{confirmed} = dh_c \times area \quad (3)$$

$$dV_{confirmed,uncertainty} = \sqrt{(dh_{c,uncertainty} \times area)^2 + (dh_c \times area_{uncertainty})^2} \quad (4)$$

For the unconfirmed lakes we only calculated elevation change and its uncertainty because the boundaries could not be determined.

4. Results

4.1 Cross-verification of subglacial lake location

Using ICESat-2, we identified 13 high confidence and 48 medium confidence active lakes (61 in total). A total of 51 of these lakes were confirmed by the ArcticDEM data (Figure 3a). Two previously identified active subglacial lakes were also identified in this study, located at the Flade Isbink Ice Cap (Willis et al., 2015) and Inuppaat quuat (Howat et al., 2015; Palmer et al., 2015). Three of five other reported active lakes were sampled by ICESat-2, but no characteristic spatial pattern of subglacial lake filling and draining was found during the ICESat-2 period, indicating that these lakes may be transient features or have been in a relatively steady state during the corresponding periods. RES data collected during 1993-2016 were analysed by Bowling et al. (2019), revealing 57 stable lakes. Of the 57 stable lakes, 39 of them were sampled by the ICESat-2 ATL11 data (within a circular buffer with a radius half the lake length derived from Livingstone et al. (2022)), but no clear elevation anomalies were found. In addition, 10 of the 61 active lakes were sampled by RES data from 2017 to 2019, but no classic flat reflections were identified. This mismatch between RES- and altimeter-detected lakes has also been reported in Antarctica (Siegert et al., 2014).

4.2 Distribution of active subglacial lakes

In total, 2494 ICESat-2 footprints sampled active subglacial lakes identified over the entire GrIS, with 27 lakes covered several times, but by only one RPT. The well-sampled subglacial lakes covered by 3-4 RPTs are located in northernmost Greenland. We adopted informal names for identified subglacial lakes (Table S2) based on the associated Greenland basin name (Mouginot et al., 2019).

Active subglacial lakes are concentrated toward the ice margin and have large upstream subglacial hydrologic catchments (Figure 3a). Three main clusters of active lakes were observed in northwestern, northern, and southwestern Greenland, corresponding to regions of significant negative surface mass balance (Khan et al., 2022) and where surface meltwater can access the bed due to limited firn and the occurrence of moulins and crevasses. This distribution is consistent with that predicted by Bowling et al. (2019), with hydrologically active lakes located near or below the Equilibrium Line Altitude (ELA). There

带格式的: 使用中文规则控制首尾字符

删除的内容: $dV_{confimred} = dh_c \times area$ (3) . $dV_{confimred,uncertainty} = \sqrt{(dh_{c,uncertainty} \times area)^2 + (dh_c \times area_{uncertainty})^2}$ (4) .

删除的内容: **3.6 Lake activity recognition** . To remove the influence of systematic vertical and horizontal offsets between ArcticDEMs, we calculated the relative height anomaly by subtracting the averaged ice-surface elevation within the lake from the buffer around it (Livingstone et al., 2019). We used the same method to calculate the relative height anomaly, and then combined the ArcticDEM and ICESat-2 periods (2009-2020) to determine the temporal patterns of lake activity. Each of the DSMs was corrected against filtered ICESat altimetry data using the metadata provided. As we calculated the relative height anomaly we used the internal accuracy of the data as a measure of uncertainty. The internal accuracy of the ArcticDEM is 0.2 m (Noh & Howat, 2015), and 0.09 m for ICESat-2 footprints (Brunt et al., 2019). .

删除的内容: **validation**

删除的内容: 15

删除的内容: 46

删除的内容: identified

删除的内容: active

删除的内容: 2a

删除的内容: An additional 10 active lakes were detected by ICESat-2 but not the ArcticDEM timeseries, an

删除的内容: d

删除的内容: 5

删除的内容: missed by ICESat-2

带格式的: 字体颜色: 自动设置

带格式的: 字体颜色: 自动设置

带格式的: 字体颜色: 自动设置

带格式的: 字体颜色: 自动设置

带格式的: 字体颜色: 自动设置

删除的内容: No

删除的内容: bright,

删除的内容: and strong

删除的内容: found

删除的内容: from analysis of RES data for the 61 active lakes identified in this study

删除的内容: Of the 61

删除的内容: were

删除的内容: However, since lakes occur at all latitudes, we infer ...

删除的内容: these

删除的内容: 2a

删除的内容: in

is a general paucity of active lakes in the southeastern sector of Greenland where high accumulation rates and thick firn limit the amount of surface-derived water that reaches the ice bed (Selmes et al., 2011), and inland sectors of Greenland, where the bed is thought to be largely frozen (MacGregor et al., 2022). In contrast, stable subglacial lakes tend to be located in northern and eastern regions above the ELA (Bowling et al., 2019). Active lakes are typically located near regions of fast ice flow (>50 m/yr) (Figure S2) and 51 of them are within marine-terminating catchments. This distribution is consistent with the spatial pattern found in Antarctica (Smith et al., 2009).

The active subglacial lakes identified in this study differ in size from those observed in Antarctica, reflecting the different topographic setting, and steeper ice-surface slopes and thus hydrologic gradients controlling the morphology of subglacial lakes (see also Bowling et al., 2019). Lake area ranges from 0.20 to 16.23 km^2, with an average area of 3.11 km^2 (Figure 2b). Approximately 25% of the subglacial lakes have an area < 1 km^2, indicating that small lakes are prevalent throughout Greenland. Only one lake situated in Basin USULLUUP SERMIA was > 10 km^2 (see Figure S3). The areas of unconfirmed lakes were comparable to those of confirmed lakes based on analysis of their diameter along the ICESat-2 tracks.

4.3 Elevation change and water budget

Ice-surface elevation range is a proxy for subglacial lake depth. By combining the elevation time-series of the ArcticDEM and ICESat-2 data to give a maximum lake depth estimation for the 51 confirmed lakes, we show that 9 lakes have a depth of less 10 m, and 27 lakes have a depth between 10 and 30 m. Only 3 lakes have a depth greater than 50 m, including one known lake located beneath the Flade Isbink Ice Cap, and the estimated depth of this lake is consistent with Liang et al. (2022) (Figure S4).

Generally, active subglacial lakes in Greenland exhibit higher elevation change rates (usually larger than 1 m/yr) than those in Antarctica. Positive temporal elevation trends were identified in 59% of the lakes detected during 2019-2020 (Figure 3c), indicating net water recharge. The absolute elevation-change rates ranged from 0.01 to 16.03 m/yr with a mean value of 3.26 m/yr. The uncertainty of the elevation-change rate generally depended on the number of footprints, the slope of the lake bed, and the acquisition time of different tracks, and ranged from 0.32 to 8.09 m/yr with a mean value of 2.76 m/yr. Hydrological basins 7.1 showed positive elevation change trends, while both positive and negative trends can be found in other basins (Figure S5).

Our ability to estimate subglacial lake volume changes depended on the location and size of the lake in relation to the ICESat-2 tracks that detected the elevation anomalies. Large lakes tended to have faster volume-change rates than small lakes (with a correlation coefficient of 0.44, $p < 0.001$), suggesting that they have a greater impact on the subglacial hydrological system (Livingstone et al., 2022). Subglacial lake volume changes exhibited the same temporal pattern as the elevation changes, with most lakes displaying a positive volume change over the observation period of ICESat-2 (Figure 3d). The absolute volume change rates ranged from 1.1×10^4 to 5.17×10^7 m^3/yr with a mean value of 7.74×10^6 m^3/yr (Table S2). Volume change rate

删除的内容: The
删除的内容: can
删除的内容: provide important information on lake depth
删除的内容: lake
删除的内容: than
删除的内容: ,
删除的内容: and o
删除的内容: depth
删除的内容: 2c
删除的内容: Lakes with both positive and negative elevation change rates during the study period were found in each basin with few exceptions.
删除的内容: The largest elevation changes tended to occur in the lake center, reducing outwards to the boundary.
删除的内容: Lake
删除的内容: spatial
删除的内容: 2d
删除的内容: k

uncertainties ranged from 4×10^4 to 1.31×10^7 m^3/yr, with a mean value of 3.82×10^6 m^3/yr. Six hydrological basins exhibited a net volume gain, with the most significant gains located in basins 6.2 and 7.1 (Figure 3d).

5. Discussion

5.1 Dynamic processes of active subglacial lakes

Variable subglacial lake activity was detected by ICESat-2 during 2019-2020 (Figure 4). Thirty-five lakes exhibited only filling or draining throughout the study period. In contrast, 6 lakes experienced at least 3 filling or draining periods during 2019-2020 (Table S2). A total net positive volume change rate of 0.10 km^3/yr was found for the detected active subglacial lakes. Recharge of these subglacial lakes is thought to be generated from geothermal heat flux, frictional heating from ice flow and surface meltwater inputs (Bowling et al., 2019). As all 61 active lakes are located near or below the equilibrium line in areas of high negative surface mass balance, we hypothesise that surface meltwater runoff that reaches the ice bed has a strong control on lake activity (see also Liang et al., 2022). However, the relationship between positive volume change rate and runoff estimates from the high-resolution Regional Atmospheric Climate Model (RACMO2.3p2) (Noël et al., 2018) revealed only a slight positive correlation (with a correlation coefficient of 0.38, $p < 0.1$). This unclear relationship might reflect the relatively coarse temporal resolution of our data during individual melt seasons (cf. Liang et al., 2022), but still provides a hint that active lakes in Greenland are at least partly recharged by surface melt.

5.2 Lake activity: fill-drain patterns

Livingstone et al. (2022) classified subglacial lake activity into 5 temporal patterns based on the ratio of filling and draining durations. They found that 3 active subglacial lakes in Greenland exhibited quiescence at high stand. To further improve the understanding of dynamic hydrological processes underneath the GrIS, we used the combination of ArcticDEM and ICESat-2 to determine the fill–drain patterns of our identified active lakes over 11 years.

The temporal resolution of the ArcticDEM varies, making it difficult to discriminate clear fill-drain patterns for all lakes. However, in total we identified 11 lakes with specific fill–drain cycles (Table S2). One lake exhibited slow filling and rapid draining (Figure 4a), two lakes exhibited slow drainage and rapid filling (Figure 4b) and 8 lakes remained filled for multiple years (i.e. quiescent at high stand) before rapidly draining (Figure 4c). We did not identify active subglacial lakes that exhibited similar rates of filling and draining or that remained drained or partially drained for multiple years (i.e. quiescent at low stand) before filling and draining. The dominance of lakes quiescent at high stand provides further support for an external threshold controlling the initiation of lake drainage in Greenland (Livingstone et al., 2022). Twenty-nine of 41 drainage events happened between May and August (Table S3), with 2 lakes draining between December and February (e.g., KONG_OSCAR_GLETSCHER02). The tendency for lakes to preferentially drain in summer also supports the idea that surface meltwater can influence or trigger drainage although there is a bias here with the acquisition data restricted to summer.

删除的内容: k
删除的内容: k
带格式的: 字体颜色: 自动设置
删除的内容: 3
删除的内容: only
删除的内容: abnormal elevation changes
删除的内容: which
删除的内容: predominantly
删除的内容: measure
删除的内容: 20
删除的内容: 3a
删除的内容: , one lake exhibited similar rates of filling and draining (Figure 3b)
删除的内容: with 15
删除的内容: quiescent at high stand
删除的内容: (Figure 3c)
删除的内容: and 3 lakes
删除的内容: quiescent at low stand (Figure 3d)

6. Conclusions

We used ICESat-2 altimetry to detect active subglacial lakes underneath the Greenland Ice Sheet and to discriminate their signal from supraglacial lake drainage patterns. Multi-temporal ArcticDEM strip maps were used to extend the timeseries, allowing us to help verify the lakes and quantify their drainage history. In total, we identified 59 new active lakes, more than 8 times the previous number. Lakes are concentrated below the ELA, and correspond with regions of significant negative surface mass balance. This spatial distribution indicates that the formation and dynamism of active subglacial lakes in Greenland is related to the ability of surface-derived meltwater to access the ice bed (i.e., little snow/firn and lots of crevasses and/or moulins). Thirteen of the subglacial lakes had an area < 1 km^2, and only one lake had an area > 10 km^2, but large lakes exhibited faster volume-change rates than small lakes, suggesting that they have a greater impact on the subglacial hydrological system. Finally, lake drainages typically occur in the summer melt season, and 8 of the 11 lakes where clear fill-drain cycles were identified displayed long-term quiescence at high stand followed by drainage, suggesting surface melt might control the initiation of subglacial lake drainage in Greenland.

There is no doubt that our inventory is incomplete, likely missing lakes in the lower-latitude regions where the ICESat-2 track spacing is large, though we used time-stamped ArcticDEM data to fill spatial gaps. Although discriminating between supraglacial and subglacial lakes remains a challenge in the detection of subglacial lakes, we demonstrate the utility of ICESat-2 for removing the influence of shallow supraglacial lakes. Our confidence in identifying subglacial lakes and their drainage patterns will increase in the future as the temporal coverage is extended by ICESat-2 and other satellite data. Future work could use our inventory to determine the impact of subglacial lakes on the wider ice sheet system, including subglacial hydrology, ice dynamics and sediment and biogeochemical fluxes.

删除的内容: surface

删除的内容: toward the ice margin

删除的内容: 15

删除的内容: 20

Author contributions

Yubin Fan performed the identification of active lakes and wrote the manuscript; Chang-Qing Ke contributed to the conception of the study and supervised the work; Xiaoyi Shen contributed to the discussion and advised on the elevation change and water budget; Yao Xiao performed ArcticDEM validation on Google Earth Engine (GEE) platform. Stephen J. Livingstone and Andrew J. Sole revised the manuscript and advised on lake confidence level classification. All authors contributed to the discussion of the results and to the improvement of the manuscript.

Competing interests

The authors declare that they have no conflict of interest.

Acknowledgements

This work was supported by the Program for National Natural Science Foundation of China (grant No. 41830105 & 42011530120). ICESat-2 data (https://nsidc.org/data/ATL11/versions/3) were obtained from the National Snow and Ice Data Center. The ArcticDEMs were obtained and processed in the GEE platform (https://code.earthengine.google.com/). RACMO2.3p2 Greenland daily runoff data were kindly provided by Brice Noël and MAR data were kindly provided by Xavier Fettweis.

References

Bessette, J. T., Schroeder, D. M., Jordan, T. M., and MacGregor, J. A.: Radar-sounding characterization of the subglacial groundwater table beneath Hiawatha Glacier, Greenland. Geophys. Res. Lett., 48, e2020GL091432, https://doi.org/10.1029/2020GL091432, 2021.

Bowling, J.S., Livingstone, S. J., Sole, A. J. and Chu, W.: Distribution and dynamics of Greenland subglacial lakes. Nature Communications, 10:2810, https://doi.org/10.1038/s41467-019-10821-w, 2019.

Brunt, K., Smith, B., Sutterly, T., Kurtz, N., & Neumann, T: Comparisons of Satellite and Airborne Altimetry With Ground-Based Data From the Interior of the Antarctic Ice Sheet. Geophysical Research Letters, 48, https://doi.org/10.1029/2020GL090572, 2021.

Datta, R. T., and Wouters, B.: Supraglacial lake bathymetry automatically derived from ICESat-2 constraining lake depth estimates from multi-source satellite imagery. The Cryosphere, 15, 5115–5132, https://doi.org/10.5194/tc-15-5115-2021, 2021.

Fair, Z., Flanner, M., Brunt, K. M., Fricker, H. A., and Gardner, A.: Using ICESat-2 and Operation IceBridge altimetry for supraglacial lake depth retrievals. The Cryosphere, 14, 4253–4263, https://doi.org/10.5194/tc-14-4253-2020, 2020.

Fettweis, X., Hofer, S., Séférian, R., Amory, C., Delhasse, A., Doutreloup, S., Kittel, C., Lang, C., Bever, J., Veillon, F., and Irvine, P.: Brief communication: Reduction of the future Greenland ice sheet surface melt with the help of solar geoengineering. The Cryosphere, 15, 3013–3019, https://doi.org/10.5194/tc-15-3013-2021, 2021.

Fricker, H. A., Scambos, T., Bindschadler, R., and Padman, L.: An active subglacial water system in West Antarctica mapped from space. Science, 315(5818), 1544–1548, https://doi.org/10.1126/science.1136897, 2007.

Fricker, H. A., Arndt, P., Brunt, K. M., Datta., R. T., Fair, Z. and Jasinski, M. F.: ICESat-2 Meltwater Depth Estimates: Application to Surface Melt on Amery Ice Shelf, East Antarctica. Geophys. Res. Lett., 48, e2020GL090550, https://doi.org/10.1029/2020GL090550, 2020.

Gray, L., Joughin, I., Tulaczyk, S. and Spikes, V. B.: Evidence for subglacial water transport in the West Antarctic Ice Sheet through three-dimensional satellite radar interferometry. Geophys. Res. Lett., 32, L03501, https://doi.org/10.1029/2004GL021387, 2005.

Howat, I. M., Porter, C., Noh, M. J., Smith, B. E. and Jeong, S.: Brief communication: sudden drainage of a subglacial lake beneath the Greenland Ice Sheet. The Cryosphere, 9, 103–108, https:// doi.org/10.5194/tc-9-103-2015, 2015.

带格式的：默认段落字体

删除的内容：Brunt, K. M., Neumann T. A., and Smith B. E.: Assessment of ICESat-2 Ice Sheet Surface Heights, Based on Comparisons Over the Interior of the Antarctic Ice Sheet. Geophys. Res. Lett., 46, 13,072–13,078, https://doi.org/10.1029/2019GL084886, 2019.

Khan, S.A., Bamber, J.L., Rignot, E., Helm, V., Aschwanden, A., Holland, D.M., Broeke, M., King, M., Noël, B., Truffer, M., Humbert, A., Colgan, W., Vijay, S., and Munneke, P.: Greenland mass trends from airborne and satellite altimetry during 2011–2020. J. Geophys. Res.: Earth Surf., 127(4), p.e2021JF006505, https:// doi.org/10.1029/2021JF006505, 2022.

Li, Y., Shi, H., Lu, Y., Zhang, Z. and Xi, H.: Subglacial discharge weakens the stability of the Ross Ice Shelf around the grou nding line. Polar Res., 40, 3377, https:// doi.org/10.33265/polar.v40.3377, 2021.

Liang, Q., Xiao, W., Howat, I., Cheng, X., Hui, F., Chen, Z., Jiang, M., and Zheng, L.: Filling and drainage of a subglacial la ke beneath the Flade Isblink ice cap, northeast Greenland. The Cryosphere Discussions, pp.1-17, https://doi.org/10.5194/tc-2 021-374, 2022.

Livingstone, S. J., Clark, C. D., Woodward, J. and Kingslake, J.: Potential subglacial lake locations and meltwater drainage p athways beneath the Antarctic and Greenland ice sheets. The Cryosphere, 7, 1721–1740, https:// doi.org/10.5194/tc-7-1721-2 013, 2013.

Livingstone, S. J., Sole, A. J., Storrar, R. D., Harrison, D., Ross, N., and Bowling, J.: Brief communication: Subglacial lake d rainage beneath Isunguata Sermia,West Greenland: geomorphic and ice dynamic effects. The Cryosphere, 13, 2789–2796, htt ps://doi.org/10.5194/tc-13-2789-2019, 2019.

Livingstone, S. J., Li, Y., Rutishauser, A., Sanderson, R. J., Winter, K., Mikucki, J. A., Björnsson, H., Bowling, J., Chu, W., Dow, C., Fricker, H., McMillan, M., Ng, F., Ross. N., Siegert, M., Siegfried, M., and Sole, A.: Subglacial lakes and their cha nging role in a warming climate. Nat. Rev. Earth Environ., 19, https://doi.org/10.1038/s43017-021-00246-9, 2022.

MacFerrin, M., Machguth, H., van As, D., Charalampidis, C., Stevens, C. M., Heilig, A., Vandecrux, B., Langen, P. L., Mott ram, R., Fettweis, X., Broeke, M., Pfeffer, W. T., Moussavi, M. S., and Abdalati, W.: Rapid expansion of Greenland's low- p ermeability ice slabs. Nature, 573, 403–407, https://doi.org/10.1038/s41586-019-1550-3, 2019.

MacGregor, J. A., Chu, W., Colgan, W. T., Fahnestock, M. A., Felikson, D., Karlsson, N. B., Nowicki, S., and Studinger, M.: GBaTSv2: A revised synthesis of the likely basal thermal state of the Greenland Ice Sheet. The Cryosphere Discussions, pp. 1-25. https://doi.org/10.5194/tc-2022-40, 2022.

Magruder, L. A., Brunt, K. M., Neumann, T., Klotz, B., and Alonzo, M.: Passive ground-based optical techniques for monitoring the on-orbit ICESat-2 altimeter geolocation and footprint diameter. Earth and Space Science. https://doi.org/10.1002/essoar.10504571.1, 2020.

Maguire, R., Schmerr, N., Pettit, E., Riverman, K., Gardner, C., DellaGiustina, D. N., Avenson, B., Wagner, N., Marusiak, A. G., Habib, N., Broadbeck, J. I., Bray, V. J., and Bailey, S. H.: Geophysical constraints on the properties of a subglacial lake i n northwest Greenland, The Cryosphere, 15, 3279–3291, https://doi.org/10.5194/tc-15-3279-2021, 2021.

Malczyk, G., Gourmelen, N., Goldberg, D., Wuite, J., and Nagler, T.: Repeat subglacial lake drainage and filling beneath Th waites Glacier. Geophys. Res. Lett., 47, e2020GL089658, https://doi.org/10.1029/2020GL089658, 2020.

Mouginot, J. and Rignot, E.: Glacier catchments/basins for the Greenland Ice Sheet." UC Irvine Dash. https://doi.org/10.728 0/D1WT11, 2019.

Noël, B., van de Berg, W. J., van Wessem, J. M., van Meijgaard, E., van As, D., Lenaerts, J. T. M., Lhermitte, S., Ligtenberg, S. R. M., Medley, B., Reijmer, C. H., Tricht, K., Trusel, L. D., van Ulft, L. H., Wouters, B., Wuite, J., and van den Broeke, M.R.: Modelling the climate and surface mass balance of polar ice sheets using RACMO2 – Part 1: Greenland (1958–2016), The Cryosphere, 12, 811-831, https://doi.org/10.5194/tc-12-811-2018, 2018.

Noh, M.J. and Howat, I. M.: Automated stereo-photogrammetric DEM generation at high latitudes: Surface extraction with TIN-based search-space minimization (SETSM) validation and demonstration over glaciated regions. GISci Remote Sens, 52, 198–217, https://doi.org/10.1080/15481603.2015.1008621, 2015.

Palmer, S. J., Dowdeswell, J. A., Christoffersen, P., Young, D. A., Blankenship, D. D., Greenbaum, J. S., Benham, T., Bamber, J., and Siegert., M. J.: Greenland subglacial lakes detected by radar, Geophys. Res. Lett., 40, https://doi.org/10.1002/2013GL058383, 2013.

Palmer, S., Mcmillan, M. and Morlighem, M.: Subglacial lake drainage detected beneath the Greenland ice sheet. Nature Communications. 6, 8408, https://doi.org/10.1038/ncomms9408, 2015.

Pope, A., Scambos, T.A., Moussavi, M., Tedesco, M., Willis, M., Shean, D. and Grigsby, S.: Estimating supraglacial lake depth in West Greenland using Landsat 8 and comparison with other multispectral methods. The Cryosphere, 10(1), pp.15-27, https://doi.org/10.5194/tc-10-15-2016, 2016.

Porter, C., Morin, P., Howat, I., Noh, M.J., Bates, B., Peterman, K., Keesey, S., Schlenk, M., Gardiner, J., Tomko, K. and Willis, M.: ArcticDEM. Harvard Dataverse, 1, pp.2018-30, https://doi.org/10.7910/DVN/OHHUKH, 2018.

Selmes, N., Murray, T., and James, T. D.: Fast draining lakes on the Greenland Ice Sheet. Geophys. Res. Lett., 38(15). https://doi.org/10.1029/2011gl047872, 2011.

Sergienko., O. V.: Glaciological twins: basally controlled subglacial and supraglacial lakes. J. Glaciol., 59, 213, https://doi.org/10.3189/2013JoG12J040, 2013.

Siegert, M. J., Ross, N., Corr, H., Smith, B., Jordan, T., Bingham, R. G., Ferraccioli, F., Rippin, M., and Le Brocq, A.: Boundary conditions of an active West Antarctic subglacial lake: implications for storage of water beneath the ice sheet. The Cryosphere, 8, 15–24, https://doi.org/10.5194/tc-8-15-2014, 2014.

Siegfried, M. R., and Fricker, H. A.: Thirteen years of subglacial lake activity in Antarctica from multi-mission satellite altimetry. Ann. Glaciol., 59(76pt1), 42-55. https://doi.org/10.1017/aog.2017.36, 2018.

Siegfried, M. R., and Fricker, H. A.: Illuminating active subglacial lake processes with ICESat-2 laser altimetry. Geophys. Res. Lett., 48, e2020GL091089, https://doi.org/10.1029/2020GL091089, 2021.

Smith, B., Fricker, H., Joughin, I., and Tulaczyk, S.: An inventory of active subglacial lakes in Antarctica detected by ICESat (2003–2008). J. Glaciol., 55(192), 573–595, https://doi.org/10.3189/002214309789470879, 2009.

Smith, B. E., Gourmelen, N., Huth, A., and Joughin, I.: Connected subglacial lake drainage beneath Thwaites Glacier, West Antarctica. The Cryosphere, 11(1), 451-467, https://doi.org/10.5194/tc-11-451-2017, 2017.

Smith, B., Dickinson, S., Jelley, B. P., Neumann, T. A., Hancock, D., Lee, J., and Harbeck, K.: ATLAS/ICESat-2 L3B Annual Land Ice Height, Version 4. Boulder, Colorado USA. NASA National Snow and Ice Data Center Distributed Active Archive Center, https://doi.org/10.5067/ATLAS/ATL11.004, 2021.

Studinger, M., Bell, R. E. and Tikku, A. A.: Estimating the depth and shape of subglacial Lake Vostok's water cavity from aerogravity data. Geophys. Res. Lett., 31, L12401. https://doi.org/10.1029/2004GL019801, 2004.

Vick-Majors, T. J., Michaud, A. B., Skidmore, M. L., Turetta, C., Barbante, C., Christner, B. C., Dore, J. E., Christianson, K., Mitchell, A. C., Achberger, A, M., Mikucki, J, A., and Pris, J. C.: Biogeochemical connectivity between freshwater ecosystems beneath the West Antarctic ice sheet and the sub-ice marine environment. Global Biogeochem. Cycles, 34, e2019GB006446. https://doi.org/10.1029/2019GB006446, 2020.

Willis, M. J., Herried, B. G., Bevis, M. G., and Bell, R. E.: Recharge of a subglacial lake by surface meltwater in northeast Greenland. Nature, 518(7538), 223-U165, https://doi.org/10.1038/nature14116, 2015.

Wright, A. P., and Siegert, M.: A fourth inventory of Antarctic subglacial lakes, Antarctic Science, 24 (6), 659–664, https://doi.org/10.1017/S095410201200048X, 2012.

Yan, S., Blankenship, D.D., Greenbaum, J.S., Young, D.A., Li, L., Rutishauser, A., Guo, J., Roberts, J.L., van Ommen, T.D., Siegert, M.J. and Sun, B.: A newly discovered subglacial lake in East Antarctica likely hosts a valuable sedimentary record of ice and climate change. Geology, 50 (8), 949–953, https://doi.org/10.1130/G50009.1, 2022.

Figures

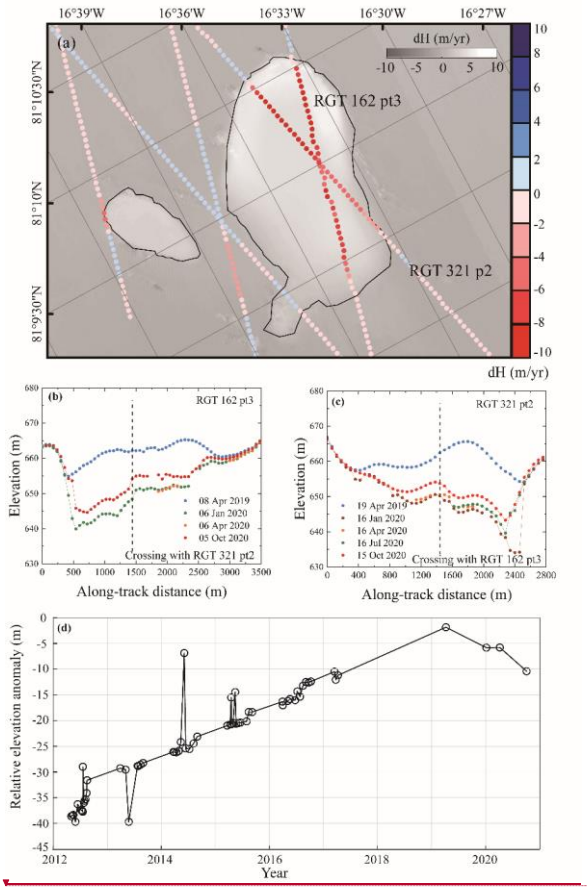

Figure 1. Active subglacial lake detection method, using Subglacial Lake ICE_CAPS_NE01 as an example. (a) The elevation change rate was derived from ICESat-2 and overlaid on the elevation difference maps between the two ArcticDEMs (20160923-20160621). The black polygons show the inferred lake boundaries derived from the ArcticDEM. The red-blue spots represent the elevation change rate derived from the linear fit of ICESat-2, while the grayscale colourbar represents the elevation change rate derived from the ArcticDEM. Elevation anomaly profiles across the subglacial lake are given for RGT 162 pt3 (b) and RGT 321 pt2 (c). The colors of the points correspond to the ICESat-2 observation times, and the vertical dashed lines show the location of the cross point. (d) Time-series of relative elevation anomaly based on the combined ArcticDEM and ICESat-2 tracks. Note the ~30 m of ice uplift over 6 years that is interpreted to be subglacial lake filling, followed by 10 m of subsidence over 1 year interpreted as slow subglacial lake drainage.

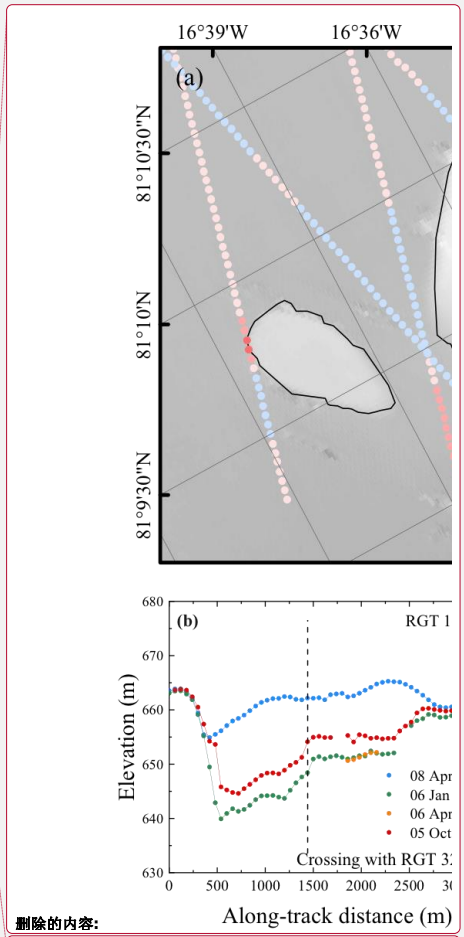

删除的内容:

带格式的: 居中

删除的内容: line

删除的内容: s

删除的内容: boundary

删除的内容: (a)

删除的内容: The red-blue colourbar stands for the ICESat-2, while grayscale colourbar stands for ArcticDEM. Elevation anomaly profiles across the subglacial lake along two ICESat-2 tracks (b) and (c)

删除的内容: Their spatial locations are also indicated in (a).

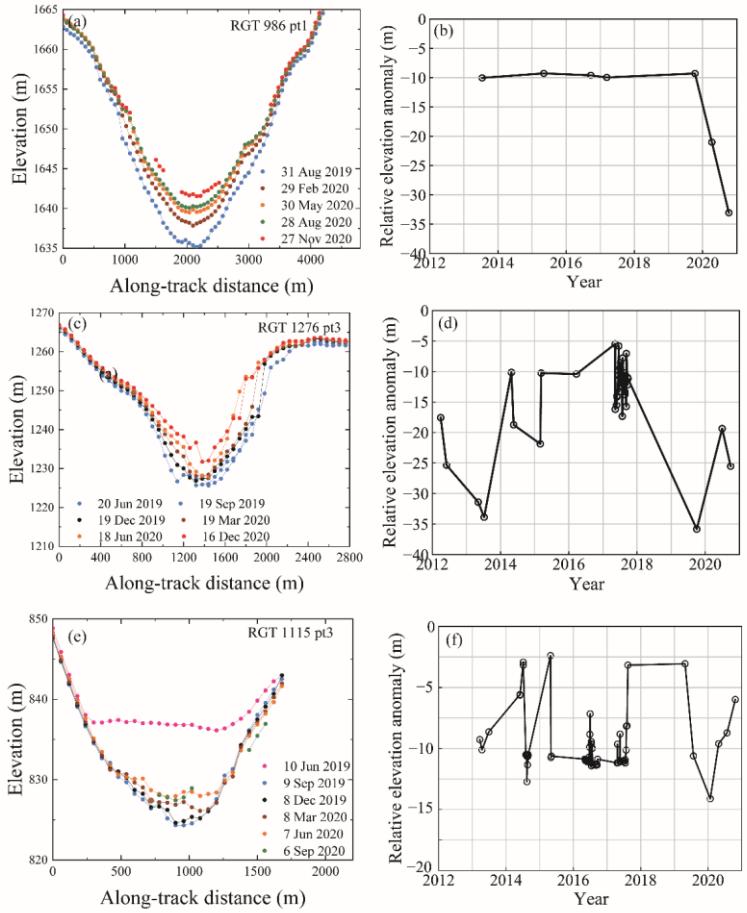

Figure 2. Examples of lake confidence level classification. The left column shows the elevation anomaly profiles across the subglacial lake derived from ICESat-2, and the right column shows the time-series elevation anomaly based on ArcticDEM and ICESat-2 tracks. The first row is the high confidence level, which exhibits >10 m ice-surface elevation change and an elevation change pattern typical of subglacial lakes (quiescent at high stand). Second row is a medium confidence level lake, which shows consistent elevation change, but with a less clear elevation-change pattern. The third row is a low confidence level lake, which contains a clear flat spot and a seasonal elevation change signal more typical of surface lakes and is therefore discounted from the inventory.

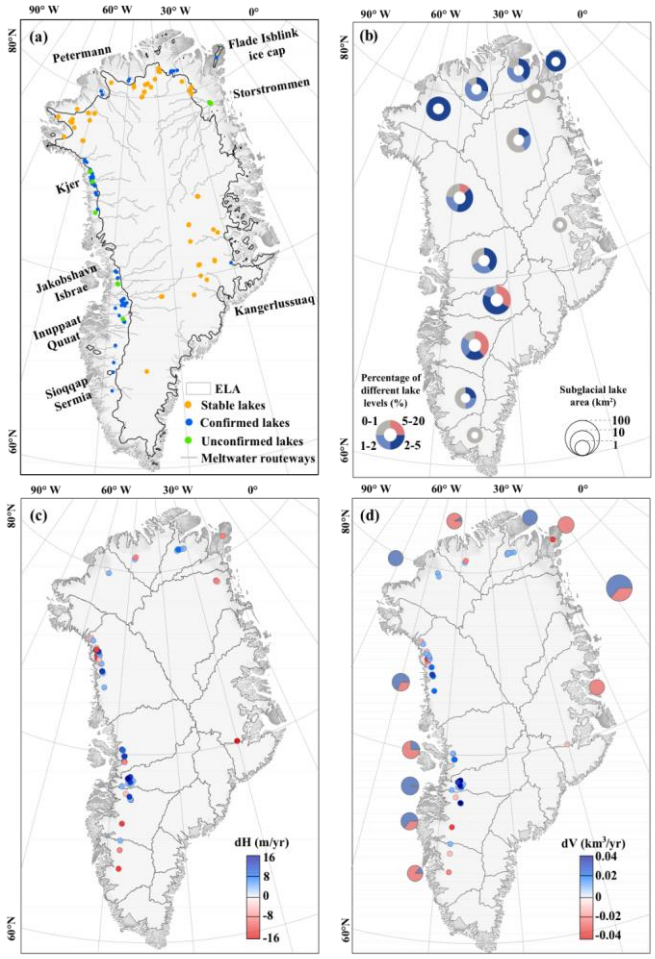

Figure 3 Maps of the (a) location, (b) area, (c) elevation change rate and (d) volume change rate for the current active subglacial lakes under the Greenland Ice Sheet. The diameter in panel (b) is scaled by the total area of the active lake, with four sections representing the number of different lake size levels. Enlarged panels for (c) and (d) can be found in Figure S5 and Figure S6 respectively. The total lake volume-change rate for each basin is shown as a circle, with the circle size is proportional to the magnitude of the absolute rate. Meltwater pathways were derived from the hydraulic gradient (Livingstone et al., 2013). The Equilibrium Line Altitude (ELA) was derived from daily MARv3.12.1 data (Fettweis, et al., 2021). Stable lakes in (a) are from Livingstone et al. (2022).

删除的内容: 2
删除的内容: (a)
删除的内容: (b)
删除的内容: (c)
删除的内容: (d)
删除的内容: the
删除的内容: The m
删除的内容: , and t
删除的内容: (a)

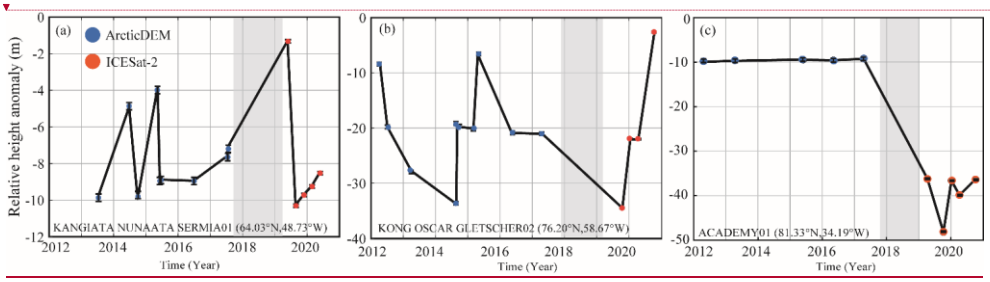

Figure 4. Time series of surface elevation change for three selected active lakes based on ArcticDEM (blue dots) and ICESat-2 tracks (orange dots). Each point represents the mean relative elevation difference between the lake and the adapted buffer derived from section 3.2: (a) mode of slow filling and rapid draining, (b) mode of slow drainage and rapid filling, and (c) modes of long-term quiescence at a high stand. Gray bar indicates the ArcticDEM/ICESat-2 data gap.

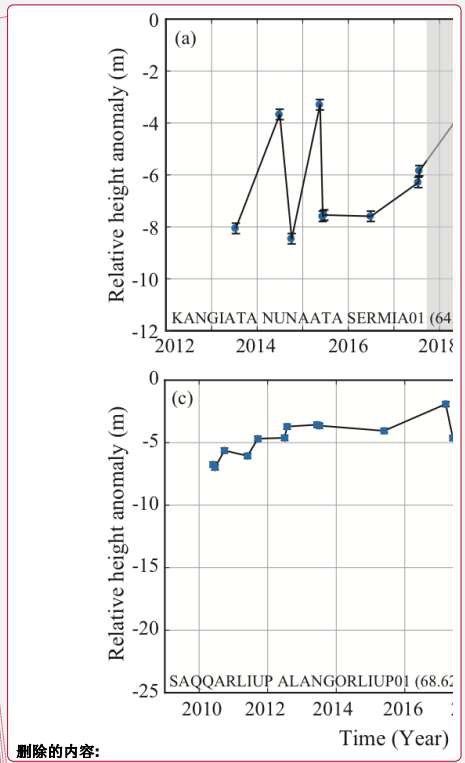

删除的内容:
删除的内容: 3
删除的内容: height
删除的内容: four
删除的内容: a 500 m buffer
删除的内容: mode of similar rates of filling and draining,
删除的内容:
删除的内容: (c) and low stand (d)